Allan Hills A81005

Anorthositic regolith breccia

31.39 g

Figure 1: Photograph of ALH A81005 as found in the Allan Hills Icefield, January 1982.

Introduction

On January 17, 1982, an interesting achondrite was found in the Allan Hills icefield by John Schutt and Ian Whillans (Fig. 1). It had a 50%, thin, tan-green fusion crust, and in the interior was exposed numerous white to grey breccia fragments. Ian and John had found what later became named, Allan Hills (ALH) A81005, the first recognized meteorite from the Moon (Fig. 2). This sample was of historic significance not only because it was the first lunar meteorite, but it became a great piece of evidence in favor of dynamic arguments that fragments of the Moon and Mars could be delivered to the Earth after being ejected from their parent bodies during an impact event (e.g., Marvin et al., 1983). The possibility that this meteorite represented material not sampled by the Luna or Apollo missions led many scientists to request pieces for detailed study. Because the meteorite was fairly small, the group overseeing the distribution of samples, the Meteorite Working Group, delayed their recommendation to ensure that distribution would be fair yet expedient.

Figure 2: Photograph of ALH A81005,0 in the Antarctic Meteorite Processing Laboratory at NASA-JSC (NASA photo S82-35869).

This process is described in some detail by Cassidy (2003), and set a precedent for how precious meteorite samples could be allocated.

Petrography and Mineralogy

ALH A81005 is a polymict regolith breccia that contains clasts of low Ti mare basalt, high Ti mare basalt, granulitic breccia, cumulate breccia, impact melt, anorthosite, norite, and troctolite. It also contains many soil components (regolith breccia and agglutinate), and mineral and glass fragments (e.g., Fig. 3 and Table 1).

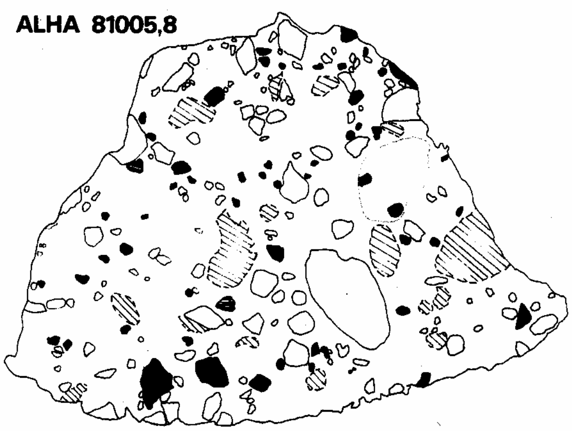

Fig. 1. Sketch of ALHA 81005,8. White = granulites; black = anorthosites and plagioclases; striped = varied impact melts. Remainder is smaller clasts and matrix. Longest dimension is about 2 cm.

Figure 3: reproduced from Ryder and Ostertag (1983) to illustrate the diversity of clast types in ALH A81005,8.

It was recognized right away that the more Fe-rich clasts bridged the gap between the Mg suite and ferroan anorthosite suite Apollo samples (Fig. 4). Some felt that this is evidence that ALH A81005 lithologies include a more evolved stage of fractional crystallization than the Apollo samples (Kallemeyn and Warren, 1983). Furthermore, FeO/MnO in pyroxenes, clearly overlap with those defined by Apollo lunar samples (Fig. 5).

Renewed studies of ALH A81005 (e.g., Treiman et al., 2008; Maloy and Treiman, 2005, 2007) have focussed on the magnesian anorthositic granulites, and the fact that they are different from any granulites in the Apollo collections, and distinct from the FAN anorthosites that are common in Apollo collection. The MAG clasts cannot be explained by mixtures of lunar mantle and FAN, nor are they easily explained as products from a magma ocean scenario. Their common occurrence in lunar feldspathic meteorites (also in Dho025, DaG400, MAC88104, and PCA02007) and therefore in the highland terrane indicates they have global significance, yet their origin is currently unknown.

Chemistry

Fractions of ALH A81005 have been analyzed by several different groups (Palme et al., verKouternen et al., Laul et al., Korotev et al., Kallemeyn and Warren, and Boynton and Hill, 1983), and although there are minor differences in composition

Table 1: Modal analysis of ALH A81005, 7 (Simon et al., 1983)

Component	#clasts	abundance
Clasts		
a) ANT (anorthosite, norite, troctolite		
Anorthosite	7	
Noritic anorthosite	1	
Anorthositic norite	2	
Anorthositic troctolite	2	
Norite	1	
Troctolite	3	
Unidentified	3	
b) Granulitic breccia	1	
c) Crystalline melt breccia	3	
d) Basalt	2	
Total	25	29.9%
Fused Soil component		
Regolith breccia		1.5
Agglutinate		5.2
Mineral Fragments		
Pyroxene and olivine		2.2
Plagioclase		8.6
Maskelynite		0.9
Opaque		0.1
Glass Fragments		
Orange/black		0
Yellow/green		0.2
Colorless		0.6
Brown		0.2
Miscellaneous		
Devitrified glass		5.8
Others		0.1
Matrix		44.7

attributable to variation in the clast types represented in the individual fragments, there are some important generalizations that can be drawn. The major, minor and trace element composition of ALH A81005 represents lunar highland material that has only a minor KREEP component (Fig. 7), and most likely comes from a source that is distant from the K-, U- and Th-enriched center of the nearside. Furthermore, K/La ratios (Fig. 6) showed that ALH A81005 has a distinctly lunar composition, plotting with the field defined by Apollo samples for these four diagnostic elements. Finally, although some groups measured very low concentrations of siderophile elements in ALH A81005, and argue for a pristine nature, there are other studies reporting quite high concentrations.

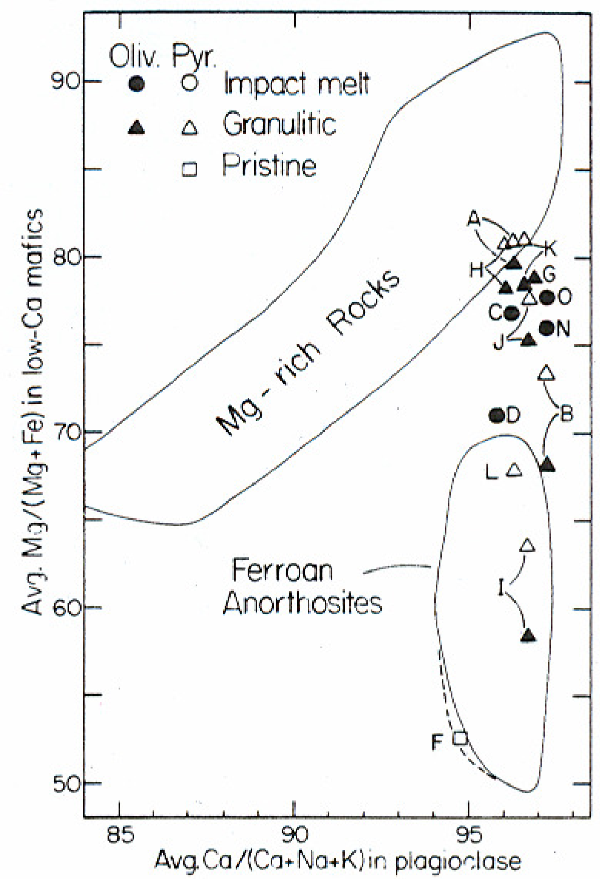

Figure 4: Mg/(Mg+Fe) in low Ca mafics vs. Ca/(Ca+Na+K) in plagioclase for clast minerals (from Kallemeyn and Warren, 1983). Letters refer to different clasts.

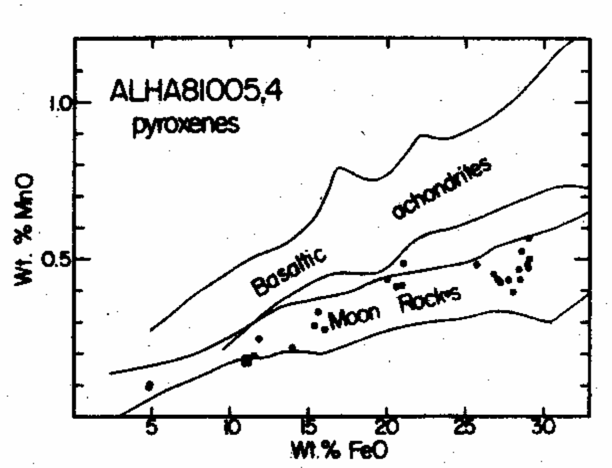

Figure 5: FeO vs. MnO for pyroxenes from ALH A81005 showing complete overlap with the lunar sample field (from Kallemeyn and Warren (1983).

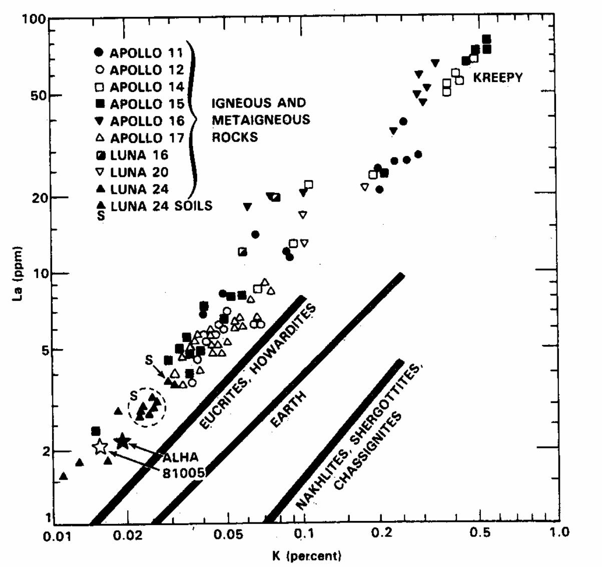

Figure 6: K vs. La for Apollo and Luna samples compared to those measured for ALH A81005 by Laul et al. (1983).

Radiogenic age dating

There has been no published Rb-Sr, Lu-Hf or Sm-Nd dating of ALH A81005, but there have been efforts to date the sample using the K-Ar and U-Pb systems. Using a linear correlation of ^{40}Ar versus ^{36}Ar (for sieved fractions of a

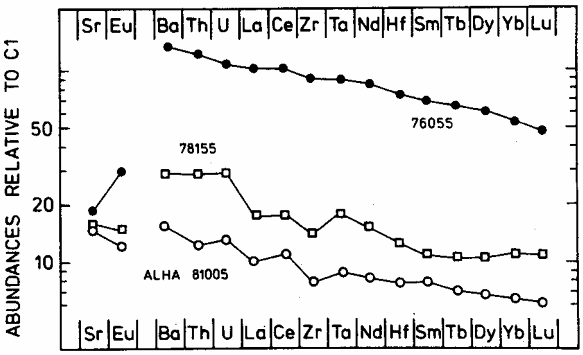

Figure 7: Incompatible trace element composition of ALH A81005 measured by Palme et al., (1983) as compared to KREEP-rich sample 76005 and highland sample 78155.

0.279 g sample) and assuming a K content of 230 ppm, Eugster et al. (1986) calculate a K-Ar age of 4300 ± 900 Ma. Measurements of U, Pb and Th on a 0.029 g sample by Chen and Wasserburg (1985) show that ALH A81005 has a low $^{204}Pb/^{206}Pb$ ratio, and high $^{238}U/^{204}Pb$ ratio and a highly radiogenic $^{207}Pb/^{206}Pb$ ratio. These ratios all support a lunar origin of ALH A81005, as can be seen by their comparison to other lunar highland samples (Fig. 8). In addition, noble gas isotopic compositions are very similar to lunar highland samples such as 65501, and the

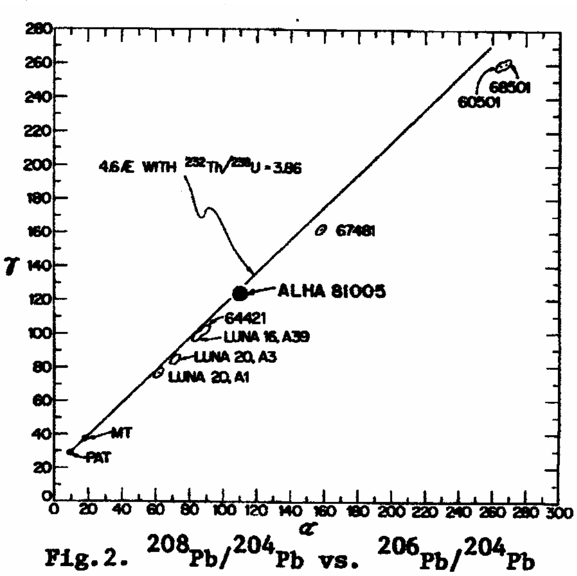

Figure 8: $^{208}Pb/^{204}Pb$ versus $^{206}Pb/^{204}Pb$ for ALH A81005 compared to Luna and Apollo high samples (Chen and Wasserburg, 1985).

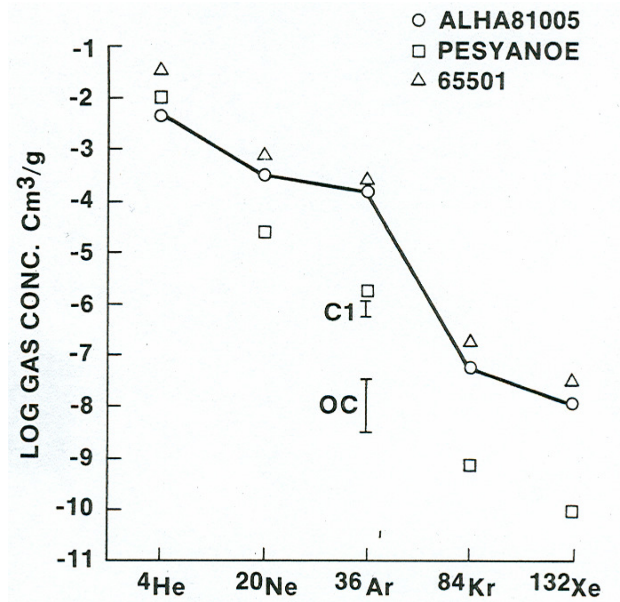

Figure 9: Noble gas isotopic compositions measured for ALH A81005, compared to highland sample 65501 (from Bogard and Johnson, 1983).

trapped Ar component suggests an age of brecciation of approximately 1 Ga (Fig. 9 and Bogard and Johnson, 1983).

Cosmogenic isotopes and exposure ages

A summary of the ejection, transfer, and terrestrial ages of some of the first few lunar meteorites, as determined by cosmogenic isotopes, was given by Eugster (1989). In this summary, Eugster shows that ALH A81005 had an ejection age of 580 Ma, a transfer age of < 100 Ka, and a terrestrial age of 170 Ka. These ages are also discussed in a broader context in the Introduction to this compendium.

Processing

ALH A81005 was processed in two main stages in 1982 and 1983 (Fig. 10 and 11). Initial and first stage processing produced splits ,1 and ,2 for thin sections and initial characterization. Split ,5 was subdivided into 11 chips for detailed geochemical and petrologic work (Fig. 12). The second stage of processing in 1983 generated two large chips containing anorthositic clasts "a" and "b", as well as many smaller chips and fines (Fig. 12). The remaining mass of ,0 currently weighs 10.783 g.

Figure 10: Stage I processing of ALH A81005 which generated splits 1, 2 and 5. Top photo is NASA S82-35865, and bottom is S82-35867.

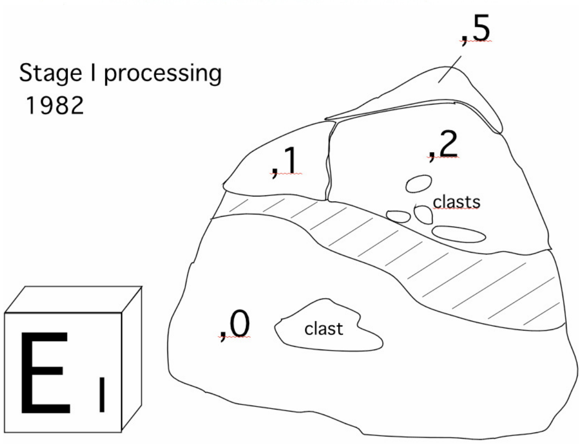

Table 2: Allocation history of ALH A81005

Split	Parent	Thin section	Wt (g)	Location	Description
2	0			subdivided	potted butt
		3	0.01	SI	thin section
		4	0.01	Terada	thin section
		8	0.01	Warren	thin section
		9	0.01	Treiman	thin section
		23	0.01	Warren	thin section
		80	0.01	Delaney	thin section
		81	0.01	Snyder	thin section
5	0		2.188	JSC	chips
7	5		0.067	JSC	potted butt
		79	0.01	JSC	thin section
10	5		0.139	Lipschutz	3 chips
11	5		0.115	Wasson	chip
12	5		0.08	Haskin	2 chips

13	5		0.081	Boynton	2 chips
14	5		0.129	Palme	4 chips
15	5		0.083	Bogard	consumed
16	5		0.117	Arnold	consumed
17	5		0.065	Herzog	2 chips
18	5		0.037	Crozaz	3 chips
19	5		0.047	Clayton	2 chips
20	5		0.029	Morris	6 chips
24	0		2.265	JSC	Chips and fines
25	0		1.14	JSC	chip with fusion crust
26	0		2.537	JSC	chips
	0	27	0.01	JSC	thin section
	0	28	0.056	Haskin	thin section
29	0		0.218	JSC	undoc chip
30	0		0.5	JSC	chips
31	0		0.205	JSC	chip with clast and fines
	0	32	0.029	Haskin	thin section
	0	33	0.005	JSC	thin section
34	0		0.002	JSC	white clast
35	0		0.002	JSC	white clast
	0	36	0.006	JSC	thin section
37	0		0.004	JSC	white clast
38	0		0.004	JSC	white clast
39	0		0.022	JSC	white clast and glass
40	0		0.079	Takeda	clast and matrix chip
	0	41	0.01	Stoeffler	thin section
	0	42	0.01	JSC	thin section
43	0		0.002	JSC	white clast
44	0		0.252	JSC	white clast and matrix
45	0		0.046	JSC	white clast
	0	46	0.01	JSC	thin section
47	0		0.036	JSC	white clast
	0	48	0.01	Treiman	thin section
49	0		0.564	JSC	chips and fines
50	0		0.212	Wasserburg	2 interior chips
51	0		0.279	Eugster	3 interior chips
	0	52	0.005	JSC	thin section
	0	53	0.007	JSC	thin section
	0	54	0.007	JSC	thin section
55	0		0.002	JSC	clast
	0	56	0.009	JSC	thin section
57	0		0.612	JSC	chips
	0	58	0.004	JSC	thin section
59	0		0.855	JSC	chips and fines
	0	60	0.004	JSC	thin section
61	0		0.162	JSC	grey clast and matrix
62	0		0.007	JSC	white clast
63	0		0.698	JSC	chips and fines
64	0		0.23	JSC	chips and fines
65	0		0.061	JSC	white clast

66	0	0.036	JSC	white clast
67	0	0.016	JSC	cabinet sweepings
69	59	0.066	Nyquist	2 chips
70	59	0.008	Maurette	chips
71	59	0.097	Oberli	chips
72	59	0.03	Pillinger	chips
73	30	0.222	JSC	chips with fusion crust
75	41	0.042	Keil	consumed
78	48	0.02	Keil	consumed
83	31	0.062	Sears	matrix rich
84	31	0.056	Sears	clast rich
85	24	0.482	Jull	interior chip
87	0	0.12	Vogt	2 documented interior chips
88	25	0.112	Zolensky	chip with fusion crust

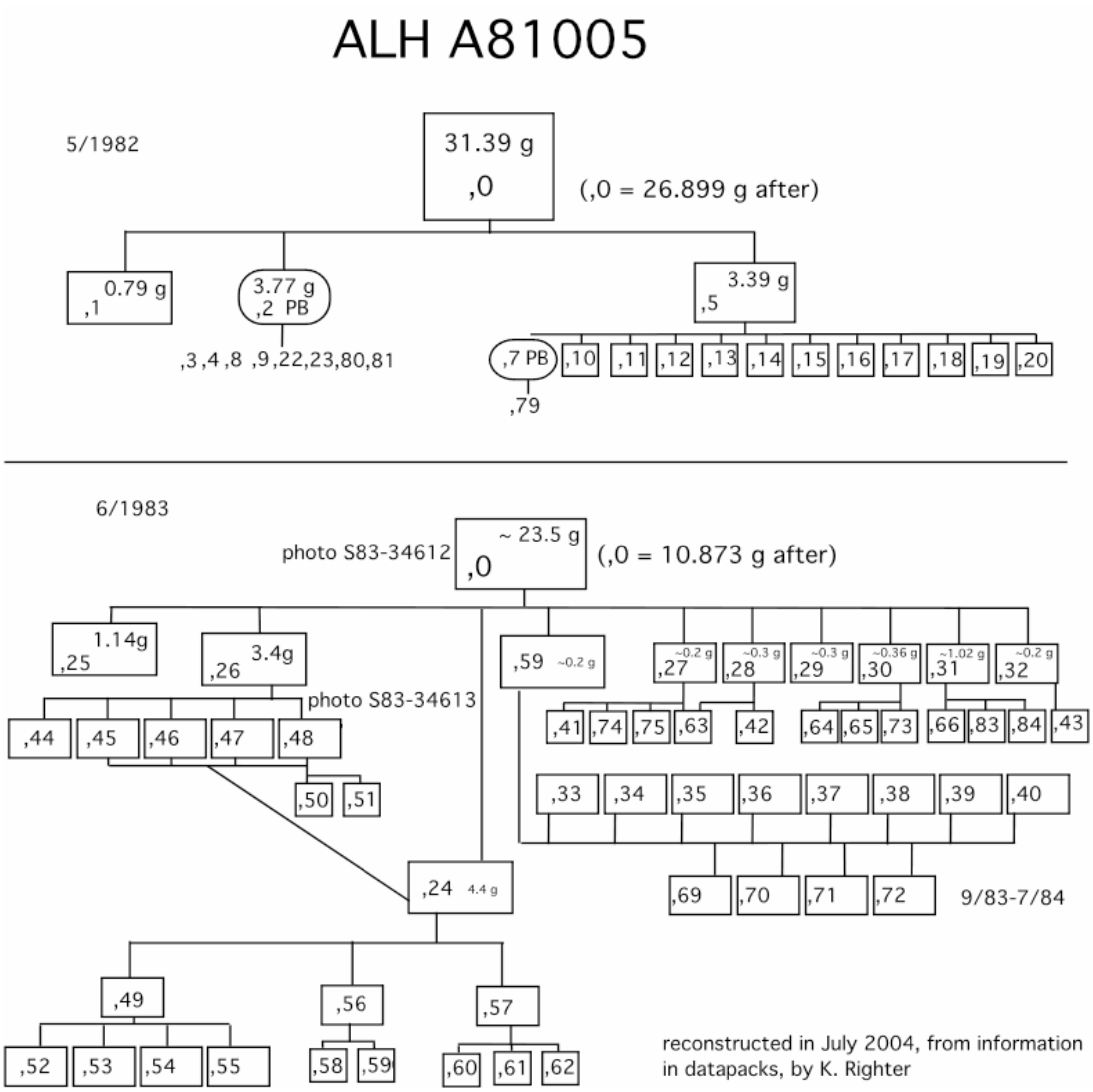

Figure 11: Genealogy of ALH A81005 showing processing in two main stages (I and II), as well as later (post 1984) processing.

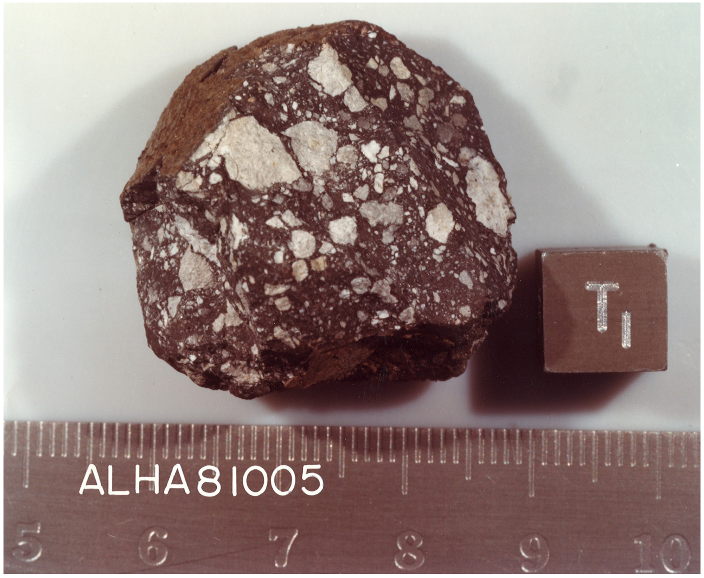

NASA photo S83-34612

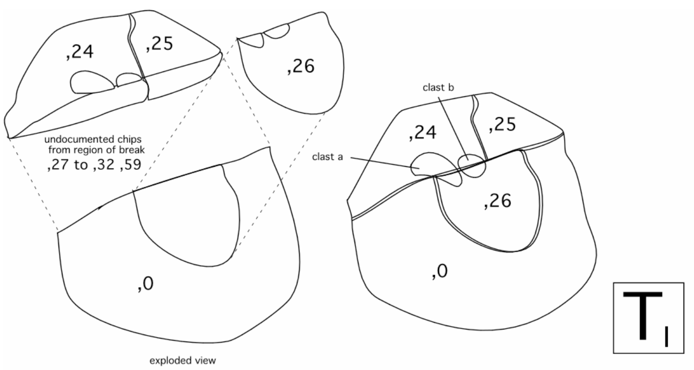

Stage II processing, 1983

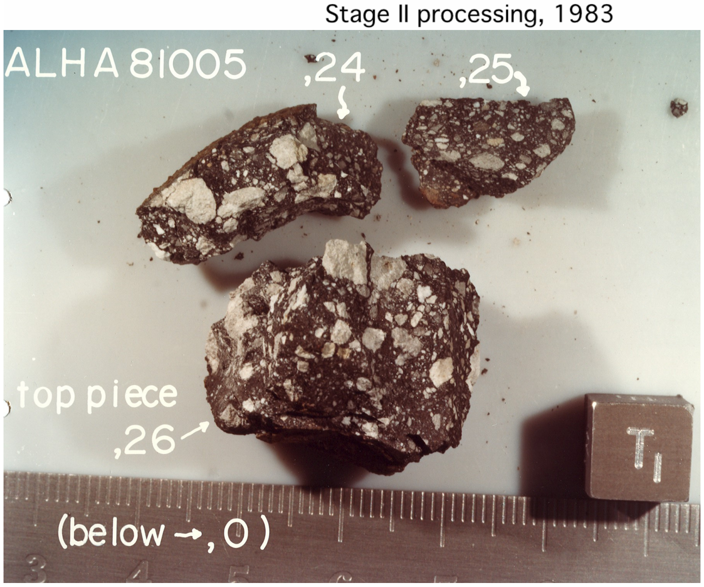

NASA photo S83-34613

Figure 12: Stage II processing which generated splits 24, 25, 26, 59 and several smaller pieces for allocations.

Table 3. Chemical composition of ALH A81005

reference	1	2	3	4	5	6	
weight	128 mg	139 mg	20.5 mg	77.71 mg	113 mg	56.6 mg	12.53 mg
				avg. of 7		A	B
method	e	f	e	e	e	e	e
SiO_2 %	46.46						
TiO_2	0.23		0.3	0.23	0.295		
Al_2O_3	25.31		26.3	25.1	26.3		
FeO	5.4		5.6	5.53	5.44	5.57	5.43
MnO	0.076		0.069	0.08	0.075	0.073	0.07
MgO	7.93		8	8.8	8.1		
CaO			15.2	14.9	14.8	14.63	14.44
Na_2O	0.3		0.31	0.321	0.3	0.28	0.3
K_2O	0.028		0.025	<0.04	0.02	0.02	0.024
P_2O_5	0.02						
S %							
sum							
Sc ppm	9.24		9.5	8.81	9	9.22	8.27
V	26		25	23	24		
Cr	862		855	900	922	901	849
Co	20.2	21.1	20	22.5	21.7	20.6	20.6
Ni	186		190	243	182	201	222
Cu							
Zn	18	4.68			5.4	5.08	5.05
Ga	2.8	2.53			2.7	2.9	2.9
Ge							
As		0.029				<0.05	0.015
Se	<0.6	0.2				0.27	<.6
Rb	<1.5	0.34		< 6	0.7	0.39	0.34
Sr	128		140	141	141	129	133
Y							
Zr	30		30	19	25	31	29.8
Nb							
Mo							
Ru							
Rh							
Pd ppb							
Ag ppb		2.4					
Cd ppb		19					
In ppb		1.5					
Sn ppb							
Sb ppb	<50	1.6				<20	1.8
Te ppb		9.2					
Cs ppm	<0.05	0.019		0.04	0.025	0.014	0.018
Ba	34		30	24	22	33	33

La	2.44		2	1.8	1.71	1.8	1.839
Ce	6.9		5	4.55	4.1	5.08	5.22
Pr							
Nd	3.9		3.3	2.75	2.9	2.88	2.99
Sm	1.18		1	0.855	0.794	0.848	0.862
Eu	0.704		0.75	0.686	0.66	0.689	0.716
Gd	1.4				0.96		
Tb	0.27		0.2	0.21	0.17	0.198	0.201
Dy	1.7		1.3		1.15	0.9	1.24
Ho	0.37				0.25		
Er					0.72		
Tm	0.18		0.13		0.11	0.121	0.12
Yb	1.06		0.86	0.705	0.69	0.812	0.827
Lu	0.15		0.13	0.113	0.106	0.119	0.118
Hf	0.92		0.7	0.63	0.61	0.696	0.695
Ta	0.12		0.1	0.079	0.07	0.098	0.095
W ppb	<130						
Re ppb							
Os ppb							
Ir ppb	7.3		6.1	7.6	6	6.4	7.3
Pt ppb							
Au ppb	2.1	2.82	2.4		1.9	1.9	2.3
Th ppm	0.35		0.32	0.198	0.26	0.327	0.336
U ppm	0.103	0.11		0.09	0.063	0.133	0.117

technique (a) ICP-AES, (b) ICP-MS, (c) IDMS, (d) Ar, (e) INAA, (f) RNAA

1) Palme et al. (1983); 2) Verkouteren et al. (1983); 3) Laul et al. (1983); 4) Korotev et al. (1983); 5) Warren et al. (1983); 6) Boynton et al. (1983)

Lunar Meteorite Compendium by K Righter 2010